

## Single-surface basis for topological particle theory

G. F. Chew

*Lawrence Berkeley Laboratory and Department of Physics, University of California, Berkeley, California 94720*

V. Poénaru

*Département de Mathématiques, Université de Paris-Sud, 91405 Orsay Cedex, France  
and Institut des Hautes Études Scientifiques, 35 route de Chartres, 91440 Bures sur Yvette, France  
(Received 26 June 1985)*

Orientations of the embellished two-dimensional bounded manifold that embeds the Feynman graph in topological particle theory (TPT) are shown capable of representing *all* discrete particle properties; there is no need for a second surface. By recognizing more fully than heretofore the patch structure of the surface, a representation is found for quark generation and lepton generation as well as for spin-chirality. "Color" is given a representation similar to that found earlier for isospin. Previously developed representations of baryon number, electric charge, and "quark" chirality remain essentially unchanged. The proposed modifications of topological particle theory leave hadron dynamics unaltered while facilitating TPT extension to electroweak interactions.

### I. INTRODUCTION

In evolution since 1978 has been a continuing effort to associate all discrete particle properties with orientations of one- and two-dimensional Feynman-graph "embellishments," with the aim of removing arbitrariness from particle theory.<sup>1-6</sup> Rather than starting with a Lagrangian, a graphical  $S$ -matrix expansion is taken as fundamental in this approach—which we call "topological particle theory" (TPT). Convergence of the topological expansion to a unitary  $S$  matrix must eventually be verified, but a generalization of Feynman's rules for topological amplitudes satisfies unitarity order by order within the expansion (Ref. 7 and Appendix C).

How are expansion components ordered? TPT extends the Feynman graph from a one-dimensional entity to something two-dimensional by embedding the graph in a surface. The reason for so "thickening" is to endow the embellished graph with an unambiguous *complexity* or "entropy." Each embellished graph is characterized by a set of non-negative integers that describe its entropy (Appendix A); when graphs are combined through connected sums, entropy cannot decrease, so components of the topological expansion may be arranged in a sequence of increasing entropy. Entropy integers such as genus stem from the topology of the embedding two-dimensional manifold; numbers of embedding dimensions higher than 2 are unsuitable for entropy bookkeeping.

The hope for convergence of the topological expansion is based on the tendency, recognized<sup>8,9</sup> in the early 1970s and now familiar in so-called "1/ $N$  expansions," for Feynman amplitudes to diminish in multiplicity with increasing entropy. For strong-interaction topologies the effective value of  $N$  has turned out in some cases to be as large as 2<sup>10</sup>, corresponding to ten two-valued orientations of Feynman-graph embellishments<sup>10</sup> (Appendix C). This paper will describe the most economical and consistent oriented embellishments so far recognized.

Two different categories of consistency requirements may be identified.

(1) Although Feynman's original expansion did not contemplate graph *contraction*—whereby certain graphs are recognized as equivalent to other graphs (contraction is often characterized as "duality")—a single term of the topological expansion represents all embellished graphs that can be contracted to the same structure.<sup>3</sup> Contractions maintain orientations together with entropy indices and control dynamics at the level of zero entropy, where amplitudes are self-generating ("bootstrap," Ref. 11 and Appendix B). A consistent set of entropy indices and associated contraction rules place severe demands on those Feynman-graph embellishments that connect with the Poincaré group; Poincaré embellishments will remain almost unaltered in this paper, although we shall slightly extend those established earlier so as to describe spin as well as chirality. But "extra-Poincaré" embellishments are less constrained by consistency with contraction, and it is here that we shall be proposing modifications.

(2) A second category of constraints arises from the need to provide a basis for classical momentum measurement. Elementary hadrons are self-generated at zero entropy, but it is necessary, in order to achieve meaning for the "asymptotic" momentum measurements on which the  $S$  matrix is based, to postulate massless photons not generated by hadrons but coupled to a conserved electric charge that can be carried by hadrons. (Reference 13 has described the generation from TPT hadron dynamics of a nonhadronic weakly interacting scalar boson that shares some characteristics of photons and thereby gives promise of a future TPT connection between the fine-structure constant and the dimensionless hadronic coupling constant.) (Stapp<sup>12</sup> has shown how classical electromagnetism emerges from coherent soft-photon collections generated through Feynman rules.) Photons must be accommodated with the same two-dimensional oriented manifold that describes hadrons, and this requirement con-

strains embellishments related to electric charge. We shall, in this paper, tamper only slightly with earlier charge-related embellishments of the Feynman graph, which required elementary photons to be accompanied by seven other elementary massless "gauge" bosons<sup>14</sup> and endowed many terms of the topological expansion with an SU(2) isospin symmetry.<sup>15</sup>

Our tampering will relate chiefly to "quark color" and "quark generation." The oriented two-dimensional manifold has no room for SU(3) color gauge symmetry; TPT accommodates no vector gluons in the sense of QCD. [Dependence of TPT on zero-entropy contractions excludes massless gauge-vector strongly interacting analogues of photons—such as the gluons of QCD. Massless gauge-vector bosons require contraction-forbidding *nonzero entropy* in spin-chiral topological structure (Appendix A).] Nevertheless, as will be seen in Sec. III, "topological quarks" have a three-valued degree of freedom reminiscent of color in pre-QCD quark models.

Both quark color and quark generation have previously been associated in TPT with a second surface<sup>3</sup>—transverse to the Feynman graph—but this paper will find a natural place for these degrees of freedom within the surface that houses all other particle features. Certain lines and patches within this surface, that previously were unoriented, will be given orientations of the kind already associated with electric charge<sup>4</sup> and with chirality.<sup>6</sup> The location of these newly oriented lines and patches decouples their orientations from Poincaré transformations and allows their interpretation as "color" and generation.

Why was it felt for so many years (since 1978) that a second, transverse, surface was needed? Historically the TPT need for color was inferred from contraction consistency *before* introduction of the lines that are now proposed as carriers of color. (These lines were introduced in 1981, not to carry color but to control chirality,<sup>6</sup> in the sense reviewed in Sec. V A.) Consistent contraction rules required an ordering of line segments incident on cubic vertices along the "belt"—the boundary of the surface that embedded the Feynman graph. A natural way to achieve such ordering was to thicken the belt into a transverse two-dimensional manifold called the "quantum surface."<sup>3</sup> A triangulation of the quantum surface, dual to the belt, then allowed association of elementary hadrons with triangulated disks on the transverse surface, and orientations of hadron-disk perimeters became interpreted as quark generation. We have thus far found no inconsistency in such a quantum-surface representation of "quark" "color" and generation and, indeed, purely strong-interaction Feynman rules remain unchanged by the representation to be proposed in this paper.

Why then might elimination of the quantum surface constitute an advance for TPT? Our motivation relates to electroweak interactions of hadrons. For "gauge" bosons the quantum surface is irrelevant, a situation that extends to leptons and to a nonhadron family of "horizontal" (H) scalar bosons predicted by TPT (Ref. 16). As a consequence there is no visible source of "quark"-generation symmetry breaking so long as this degree of freedom resides on the quantum surface. Our proposal to locate quark generation on the same surface as leptons and H

bosons opens the door to quark-generation mixing and symmetry breaking.

The proposals of the present paper, furthermore, are economical. Beyond representing color and quark generation, the quantum surface has never proved to be very useful. All interesting action has occurred on the "classical" surface housing the Feynman graph. Entropy indices, for example, have derived exclusively from the classical surface. The threeness of "color," which heretofore has been associated with quantum-surface triangles,<sup>3</sup> equally well associates with the classical-surface feature that all non-trivial vertices along the belt are cubic. We shall recognize in Sec. III that representation of "color" gives a new meaning to quark triality:  $3=1+2$ , where 2 is the number of orientations of a "color" carrying line and 1 is the number of Feynman lines close to a belt cubic vertex.

Also worth anticipating in this introduction is that the representation to be proposed for quark generation is parallel to that for lepton generation while at the same time being distinct. There are four "quark" generations in one to one correspondence with four lepton generations and mechanisms for symmetry breaking are similar. Mixing lepton generations will nevertheless be impossible, while mixing quark generations appears as an option.

## II. FEYNMAN AND FINKELSTEIN LINES; MOMENTUM AND ELECTRIC CHARGE

In TPT any open connected Feynman graph  $F$  with  $N$  external lines (carrying momentum in the usual sense) is embedded in a two-dimensional bounded, connected, oriented surface  $\Sigma$  with  $F$  ends located along the surface boundary  $\partial\Sigma$  at separate points  $e_i$ ,  $i=1, \dots, N$ . We shall denote an  $F$  line as  $f$ . The surface  $\Sigma$  has in previous literature been called the "classical surface." The (closed) one-dimensional  $\partial\Sigma$  decomposes into disconnected "external" and "internal" parts. The external part we shall refer to as the "belt," following the terminology of Ref. 3. Internal parts of  $\partial\Sigma$  touch no  $F$  ends but relate to internal  $f$ 's in a way to be described in Sec. IV. The belt decomposes exhaustively into connected particle portions  $\pi_i$ , each  $\pi$  housing within its interior (not at a  $\pi$  end point), exactly one  $F$  end, i.e., an elementary particle  $i$  belongs to a  $\pi_i$  which includes  $e_i$ .

Forthcoming embellishments of  $\Sigma$  will decorate each  $\pi$  so as uniquely to establish a particle type. This section will review the charge decoration of  $\pi$ 's for elementary mesons and gauge bosons as an illustration of general TPT principles related to momentum and electric charge.

Figure 1 shows how a three-meson, single-vertex  $F$  is embedded in an oriented disk whose circular belt (here the entire  $\partial\Sigma$ ) divides into 3  $\pi$ 's, each  $\pi$  containing one  $e$ . Notice that  $F$  embedded within an oriented  $\Sigma$  implies a cyclic ordering of  $f$ 's incident on any  $F$  vertex.

When a graph  $F$  is built by a connected sum of two other graphs  $F'$  and  $F''$ , there is a corresponding connected sum of the embedding surfaces

$$\Sigma = \Sigma' \# \Sigma''$$

made by identifying and erasing certain segments of the  $\pi_i'$  and  $\pi_i''$  (within  $\partial\Sigma'$  and  $\partial\Sigma''$ ) that belong to an inter-

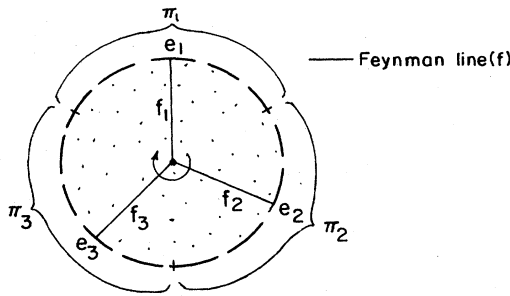


FIG. 1. Single-vertex, 3-meson Feynman graph embedded in a disk.

mediate Feynman line  $f_i$ . The identification, called a "particle plug," is made so as to perpetuate the global orientation of  $\Sigma$  and also those local orientations, to be described in the course of this paper, that establish particle identity. Figure 2 shows how global  $\Sigma$  orientation is perpetuated when two cubic meson vertices are connected by a single intermediate meson  $\pi'_i \leftrightarrow \pi''_i$ . In this example the entire  $\pi'_i$  identifies with the entire  $\pi''_i$ . Generally we require some segment from each "half" of a  $\pi$  to be identified and erased in a particle plug, recognizing that  $e_i$  divides any  $\pi_i$  into two halves. (The possibility that certain segments of  $\pi_i$  not be identified and erased in a particle plug will be related in Sec. V to Lorentz transformations and the attendant nonconservation of particle spin and chirality.) The plugging rule is to *mismatch*, in identified segments of  $\partial\Sigma'$  and  $\partial\Sigma''$ , the orientations *induced* by the respective  $\Sigma'$  and  $\Sigma''$  orientations. Feynman end points  $e'_i$  and  $e''_i$  are always identified and erased in a plug of particle  $i$ .

The global orientation of  $\Sigma$  implies alternating  $+, -$  indices on successive belt segments, as we shall see immediately below. The plugging mismatch rule then translates into a rule that  $+$  segments of the belt are to be identified with  $-$  segments. The relation between  $+$  and  $-$  boundary segments is like that between particle and antiparticle or between an "ingoing" and "outgoing" particle. Both these notions in TPT connect with the global  $\Sigma$  orientation.

We have noted how Feynman's momentum-transporting graph  $F$  divides each  $\pi$  into two halves; further boundary segmentation results from oriented lines, beginning and ending on the belt and not crossing  $F$  or each other, that were proposed by Finkelstein and collaborators<sup>4</sup> in order to represent electric charge. Here we shall denote a Finkelstein line by the symbol  $\tau$ , because these lines subsequently become recognized as the TPT repository of isospin.<sup>15</sup> Figure 3 adds  $\tau$ 's to Fig. 1 and

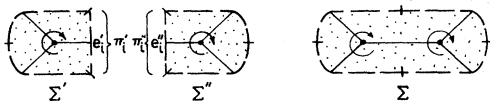


FIG. 2. Single-meson connected sum of two single-vertex disks.

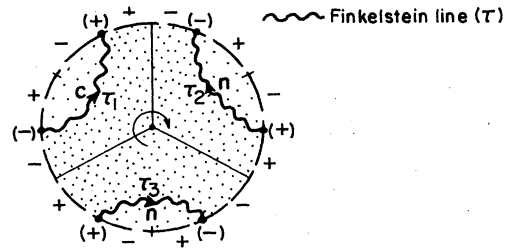


FIG. 3. Finkelstein-line embellishment of the Fig. 1 disk. (The shading will be explained by Fig. 15.)

thereby carves the belt into a total of 12 segments. We have attached  $(+, -)$  indices to these segments according to the rule that, following the sense of the global  $\Sigma$  orientation, any boundary segment immediately following a point of  $F$  contact has a  $(-)$  index. This rule is general and we shall generally use the symbol  $\beta$  for any segment of  $\partial\Sigma$ . In Fig. 3 there are  $6\beta^-$ 's and  $6\beta^+$ 's.

The orientation of each  $\tau$  allows algebraic characterization by a two-valued index defined by comparing  $\tau$  orientation to  $(+, -)$  labels induced on the  $\tau$  ends by  $\Sigma$  orientation in conjunction with  $F$ . Following the sense of  $\Sigma$  orientation along the belt, the first  $\tau$  end encountered after an  $e$  carries a  $(-)$  label, with subsequent alternation of  $(+, -)$  labels on  $\tau$  ends along the belt. If the two ends of a  $\tau$  locate on the *same* belt component (as in Fig. 3), they necessarily carry *opposite*  $(+, -)$  labels, because of the rule that no  $\tau$  crosses any other line within  $\Sigma$ . If the two ends of a  $\tau$  locate on *different* belt components (as in Fig. 4), we *require* location such that the  $(+, -)$  labels be opposite. A  $c$  index is attached to a  $\tau$  whose orientation is directed from its  $(-)$  end toward its  $(+)$  end; otherwise we give the  $\tau$  an index  $n$ . In particle plugs  $\tau$  orientation is continuous, so the  $(c, n)$  index corresponds to two conserved quantum numbers.

The  $(c, n)$  index is transferrable to certain  $\beta$ 's along the belt which touch  $\tau$  ends. The  $(c, n)$  index transfers from a  $\tau$  end to the contacting  $\beta$  whose  $(+, -)$  label agrees with

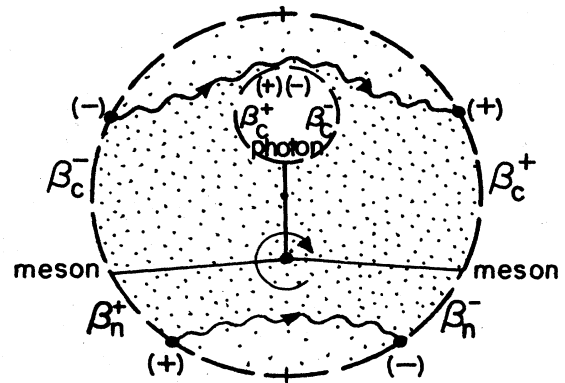


FIG. 4. Embellished Feynman graph for photon interaction with pair of charge mesons.

that of the  $\tau$  end. Any  $\beta_c^\pm$  can be said to carry  $\pm 1$  unit of electric charge while  $\beta_n^\pm$  is electrically neutral; total electric charge is thus the number of  $\beta_c^+$  minus the number of  $\beta_c^-$ .

The reason a  $\beta_c^\pm$  can be described as “charged” is that only such  $\beta$ 's couple to photons; a photon  $\pi$  consists of  $\beta_c^+$  and  $\beta_c^-$ , as shown in Fig. 4 where a photon couples to a pair of charged mesons. Here the photon occupies an entire (closed) two-segment disconnected component of the belt while each meson occupies a four-segment (open) belt portion. Appendix A reviews the status of Fig. 3 within the topological expansion, and Ref. 17 deals with Fig. 4. Here we invoke these special topologies, without explanation, as simple examples of general principles.

Reference 15 explains that the orientation of each  $\tau$  in Figs. 3 and 4 is independently reversible, so each meson and gauge boson carries an ordered pair of  $(c, n)$  labels—each such particle corresponding to the element of a  $2 \times 2$  matrix in charge space. One may say more generally that isospin has been topologized; Ref. 15 shows SU(2) isospin symmetry to be a feature of any Feynman amplitudes whose topology permits reversibility of individual Finkelstein orientations. In TPT *all* internal symmetries and quantum numbers are analogously to be understood—as will emerge from what follows.

A topological quark or antiquark is usefully defined as a  $2\text{-}\beta$  continuous belt interval divided at its midpoint by a  $\tau$  and touched at exactly one end by  $F$ , as shown in Fig. 5. Each “quark” or “antiquark” carries a  $c$  or  $n$  label (i.e., has isospin  $\pm \frac{1}{2}$ ). (The meaning of fractional electric charge for TPT “quarks” has been discussed most recently in Ref. 18.)

An elementary meson, such as appears in Figs. 3 and 4, belongs to a  $\pi$  which is a quark attached to an antiquark by an  $e$ . See Fig. 6. The belt of Fig. 3 is composed of three such meson  $\pi$ 's while one of the two disconnected components of the belt in Fig. 4 consists of two meson  $\pi$ 's.

We have associated the electric charge (isospin) of a quark with *one* of its two halves—the half that touches  $F$ . Such a segment of  $\partial\Sigma$ —touching an  $f$  at one end and a  $\tau$  at the other—we shall designate as a “fermion unit,” called  $\phi_i$ , in anticipation of Sec. V which shows that any  $\phi$ , isolated in Fig. 7, carries spin  $\frac{1}{2}$  as well as isospin.

The gauge boson of Fig. 4 (discussed at length in Ref. 17) combines  $\phi^+$  and  $\phi^-$  units together with the intervening  $e$ ; a quark (Fig. 5) combines a  $\phi$  with one other  $\beta$  (to

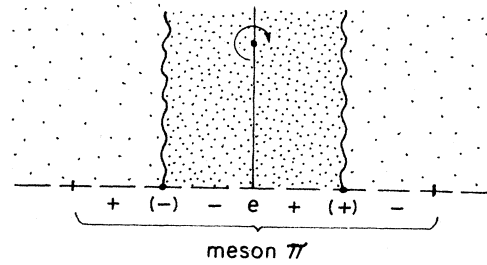


FIG. 6. Four-segment,  $q\bar{q}$ , belt portion corresponding to a meson.

be given a name in Sec. IV) but does *not* include an  $e$ . Because they do not carry momentum, quarks are not particles. Any particle has an  $e$  inside its  $\pi$ .

We remark that the  $\tau$  bisecting a quark may be called a “quark line,” although it does not carry momentum. Readers may have noted how in Fig. 3  $\tau$ 's occupy the position of Harari-Rosner quark lines.<sup>19</sup>

Because of  $f$  and  $\tau$  continuity,  $\phi^+$ 's always plug into  $\phi^-$ 's, and we may identify a conserved fermion number  $f$  which is the number of  $\phi^+$ 's minus the number of  $\phi^-$ 's. Fermion number is zero for mesons and gauge bosons but will not be zero for baryons and leptons. For all hadrons, the quark number is equal to the fermion number since fermion units in hadrons appear exclusively as “halves of quarks.” We further remark in anticipation of Sec. IV that fermion ( $\phi$ ) units of  $\partial\Sigma$  constitute the exclusive TPT repository of spin and chirality. All other boundary units carry zero spin and may be described as “bosonic.”

This section has introduced no changes in previous TPT but merely given some new language to describe existing features. The new language is appropriate to changes that will follow. In anticipation of one such change we now independently orient each  $f$  as well as each  $\tau$ . Such an orientation has previously been thought to be physically meaningless—merely telling the direction of flow of four-momentum  $p_\mu^i$  attached to the line. Reversing the orientation of  $f_i$  can be compensated by changing  $p_\mu^i$  to  $-p_\mu^i$ . Nevertheless, with a  $p_\mu^i$  and an orientation attached to each  $f_i$ , continuity of Feynman orientation in particle plugs relates to momentum conservation in a sense similar to that by which continuous Finkelstein orientation relates to charge conservation. (An important difference is that no vertices occur along  $\tau$ 's.) Furthermore simultaneous reversal of *all*  $f$  orienta-

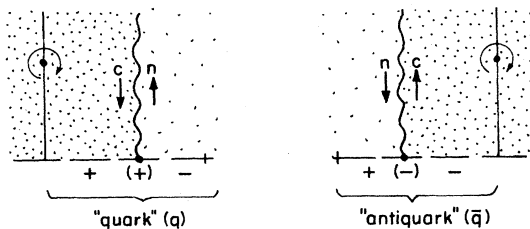


FIG. 5. Two-segment belt portions corresponding to “quark” and “antiquark.”

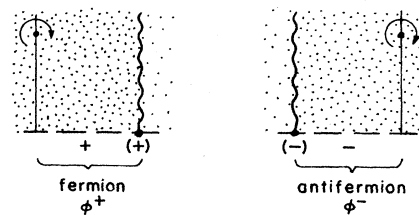


FIG. 7. Fermionic belt segments.

tions corresponds to  $TCP$ ; one may now identify this symmetry as topological (Appendix D). Henceforth every  $f$  as well as every  $\tau$  is to be understood as oriented.

### III. JUNCTION LINES AND "COLOR" LINES; BARYON NUMBER AND LEPTON NUMBER

The surface  $\Sigma$  generally is "feathered"—locally a bounded smooth surface but with a finite number of *junction lines*  $J_j$ . Appendix C reviews the TPT consistency consideration that requires junction lines. A junction line can be either a (bounded) segment, with ends on the belt, or a circle within the  $\Sigma$  interior, and along such a line three pieces of smooth surface meet. When  $\Sigma$  is disconnected along its junction lines it becomes decomposed into a number of connected smooth "sheets"  $S_k$ ; junction lines lie along sheet boundaries  $\partial S_k$  which generally are built from portions of  $\partial\Sigma$  plus junction lines. Each  $S_k$  has an orientation unambiguously correlated with that of other sheets by demanding a unique *induced* orientation for each junction line. Figure 8(a), which omits Finkelstein lines, shows the global orientation of a three-sheeted  $\Sigma$  with a single junction-line segment, embedding a baryon-antibaryon-meson single-vertex Feynman graph. Figure 8(a) can be misleading either by implying that  $\Sigma$  is embedded in a three-dimensional manifold, or that there is cyclic ordering of the three sheets meeting at a junction line. Figure 8(b) is more accurate—showing that  $J$  segments along the boundaries of each of three sheets are to be identified, but without any immediate cyclic ordering. (A cyclic ordering will be effectively provided by "color" lines described below.) Figure 8(b) also locates Finkelstein lines; in this example there are four (Harari-Rosner) "quark" lines together with one additional  $\tau$  "close to" the junction line and touching the ends of the baryon and antibaryon  $f$ 's. This extra Finkelstein line, an example of a type to be denoted  $\tau_J$ , is motivated immediately below; Appendix B gives a further reason for this  $\tau_J$  while explaining the different shading of patches in Fig. 8(b). Figure 8 illustrates the general rule that no lines (within the  $\Sigma$  interior) ever touch a junction line.

Those four oriented lines in Fig. 8(b) that each connect a boundary point to a *trivial* vertex inside  $\Sigma$ , are called "momentum-copy" lines  $f_c$ . Each junction-line end  $j$  is accompanied by the ends of exactly two  $f_c$ 's and exactly one  $e$ , as shown in Fig. 9. A belt segment  $\beta$  separates  $j$  from the ends of each of these accompanying lines. Notice how, in the  $j$  neighborhood, distinction between  $f$  and  $f_c$  is provided by the  $\tau_J$ —which contacts  $f$ .

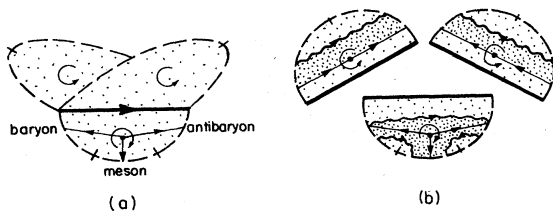


FIG. 8. (a) Single-vertex, meson-baryon-antibaryon Feynman graph embedded in a feathered surface. (b) Embellishment of the surface of (a) with Finkelstein and "color" lines.

Momentum-copy lines transport neither momentum nor electric charge but each  $f_c$  plays a role parallel to that of an associated  $f$ . Almost all statements about an  $f$  in Sec. II above apply also to an  $f_c$ . The exception is the rule that each particle  $\pi$  contains exactly one  $e$ . A  $\pi$  may contain 0, 1, or 2  $j$ 's and, correspondingly, 0, 2, or 4  $f_c$  ends. In Fig. 8 the meson  $\pi$  contains no  $j$ 's or  $f_c$  ends, while baryon and antibaryon portions of  $\partial\Sigma$  each contain a single  $j$  and 2  $f_c$  ends. The reason no  $\pi$  can contain more than 2  $j$ 's is that each  $j$  is separated by a single boundary segment from exactly 1  $e$ . An  $e$  can be adjacent to at most 2  $j$ 's.

Let us pause here to expand on the useful notion implied by the foregoing that the belt is a closed *graph* with cubic and trivial vertices joined by  $\beta$ 's. The cubic vertices coincide uniquely with  $j$ 's. Any end of a  $\tau$ ,  $f$ , or  $f_c$  lying along the belt coincides with some trivial belt vertex. Additional trivial vertices occur at dividing points between adjacent hadron belt portions where a "quark" connects with a "mated antiquark." The belt graph corresponding to Fig. 8(b) is shown in Fig. 10, where line ends are indicated by line symbols. Here there are 2 cubic vertices and 19 trivial vertices.

Along any belt branch which lies along the boundary of a single sheet,  $(+, -)\beta$  indices alternate according to the rule of Sec. II, but the 3  $\beta$ 's touching the same cubic vertex all carry the same  $(+, -)$  label, which associates with the  $j$  located at that vertex. The induced orientation of a junction line points from a  $j^{(-)}$  toward a  $j^{(+)}$ , as shown in Fig. 10 together with the induced belt orientation. The reader should remember that the junction line is *not* part of the belt but lies within the interior of  $\Sigma$ .

Section II introduced the notion of "quarks" and of fermion units of  $\partial\Sigma$ . Let us here add the notion of a *Y unit* (see Fig. 9)—which includes 3  $\beta$ 's joined by a  $j$ , together with end points of each  $\beta$  where either a  $\tau$  or an  $f_c$  impinges. As in defining quark and fermion units, we do *not* include an  $e$  within a *Y unit*. The  $\partial\Sigma$  of Figs. 8 and 10 may then be described as built from a  $Y^+$  and  $Y^-$ , 4  $q$ 's, 4  $\bar{q}$ 's, and 3  $e$ 's.

Figure 11 shows the  $(3q, Y^-) - \pi$  belonging to an elementary baryon. Here we do not show the (two-dimensional) neighboring interior of  $\Sigma$ , as we did in Fig. 6 for the meson  $\beta$ , but indicate the global orientation of  $\Sigma$  by the  $(-)$  label on the  $j$ .

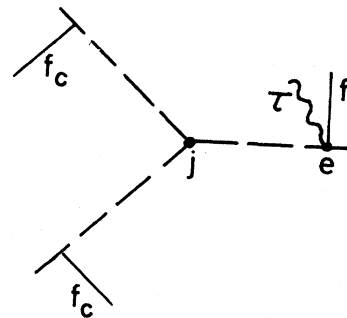


FIG. 9. Location of "color" line ends along the belt.

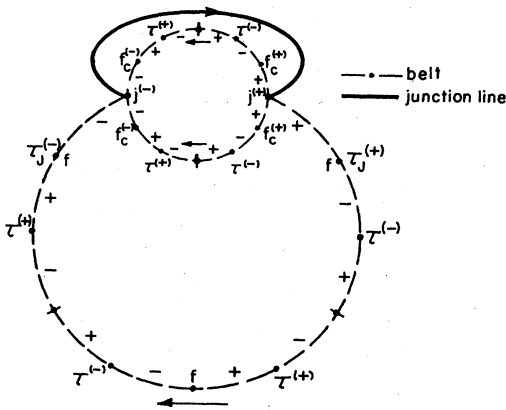


FIG. 10. The belt of graph for Fig. 8(b), with attached junction line.

As explained at the end of Sec. II, the  $f$  orientation in Fig. 11 could be assigned in either sense, but we require as a new feature of TPT (exemplified by Fig. 11) that the two  $f_c$ 's arriving near the end of any junction line be oppositely oriented. A two-valued index generally attaches to each  $f_c$  in a sense similar to that of the  $(c, n)$  index on a  $\tau$ ; this index will be transferrable to certain "quarks" where it will be described as "quark color." Let us now make precise the definition of topological color.

Lines  $f_c$  are admitted only in continuously oriented sequences that end on the belt adjacent to  $j$ 's. We shall call such a sequence of  $f_c$ 's a "color line." The end of a color line inherits a  $(+, -)$  label from the  $j$  which it accompanies and we require the two ends of the same color line always to carry opposite  $(+, -)$  labels. An index No. 2 is attributed to a color line whose orientation is directed from  $(-)$  toward  $(+)$ . Otherwise the color line carries index No. 3. Each  $j$  is accompanied by the ends of exactly one No. 2 and one No. 3 color line, as in Fig. 12.

If a quark touches  $F$  we say it carries "color" No. 1. If it touches an  $f_{c,2(3)}$  we say the quark carries color No. 2

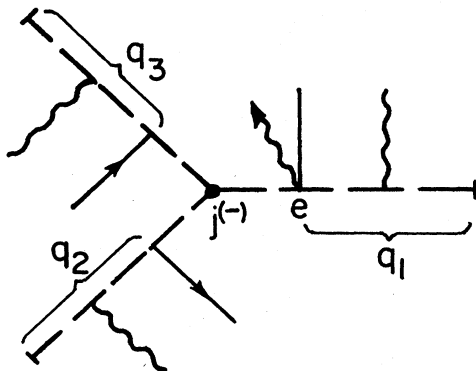


FIG. 11. Baryon belt portion (9 segments, comprising 3 "quarks" plus a  $Y^-$ ).

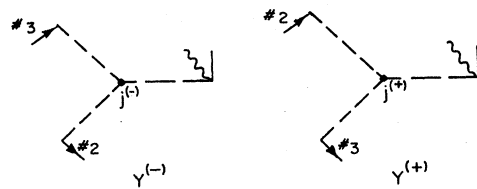


FIG. 12. Y units of the belt.

(No. 3). These "quark color" assignments are illustrated in Fig. 11. Every quark carries one of three colors.

The consistency of the foregoing requires that  $f_c$  orientation be continuous in particle plugs as well as at (trivial) vertices along color lines inside  $\Sigma$ . Conserved color quantum numbers are implied, but we shall see below that they are redundant with baryon and lepton number conservation. It is never possible independently to reverse  $f_c$  orientations, so there is no  $SU(2)$  [or  $SU(3)$ ] color symmetry. However, simultaneous reversal of all  $f_c$  orientations, amounting to a global  $2 \leftrightarrow 3$  color transformation, is a symmetry of strong-interaction topologies.

The Y plugging rule formulated in Ref. 5 is to be maintained. This rule recognizes a  $Y^+$  or  $Y^-$  belt unit attached to each end of a junction line, as shown in Fig. 12, with the three legs of each Y being distinguishable. Leg No. 1 touches the coincident ends of two lines from the interior of  $\Sigma$  while opposite orientations of single incident lines distinguish legs No. 2 and No. 3. A plug identifies  $Y^+$  with  $Y^-$  so as to achieve continuity of all four line orientations. At the end of leg No. 1, where two oriented lines impinge, the Y plug maintains orientations of tangent lines in the sense of Fig. 13.

Although never crossing  $f$ 's or  $f_c$ 's,  $\tau$ 's may thus have points of tangency. Reference 5 describes how  $q\bar{q}$  plugs are made independently of Y plugs, not necessarily preserving quark color. Quark color switching is allowed.

Consistent contraction rules require distinguishability for all three legs of a Y. Heretofore TPT has employed the transverse quantum surface to define colors No. 2 and No. 3; no orientation has previously been given either to  $f$ 's or  $f_c$ 's. Adding these orientations and the Finkelstein-Feynman points of contact near junction lines are the only changes of Feynman-graph embellishment so far presented in this paper.

The number of  $Y^+$  belt units minus the number of  $Y^-$  units is an absolutely conserved quantum number which has been called "boson number" and designated by the

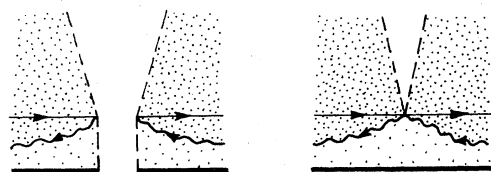


FIG. 13. Identification of Y legs in a connected sum.

symbol  $b$  (Ref. 20). Baryon number  $B$  is related to fermion number  $f$  and boson number  $b$  by the formula

$$B \equiv \frac{1}{2}f + \frac{1}{2}b. \quad (1)$$

Inspection of Fig. 11 shows a baryon to have  $f = +3$  and  $b = -1$ , so  $B = +1$ , while according to Fig. 4, mesons and gauge bosons have  $b = f = 0$  and hence  $B = 0$ . It is proposed in Ref. 17 that a lepton  $\pi$  is  $Y^+\phi^-$ , Fig. 14, with  $f = -1$  and  $b = +1$ , so leptons also have a zero baryon number. Figure 14 corresponds to the definition of lepton number

$$L \equiv \frac{3}{2}b + \frac{1}{2}f. \quad (2)$$

The  $\pi$  of Fig. 14 is seen to have  $L = +1$ , while all hadronic  $\pi$ 's have  $L = 0$ .

Continuity of "color" lines implies conservation of "color" quantum numbers but each unit of boson number  $b$  is accompanied by exactly one unit of each "color." Therefore conservation of

$$b = L - B \quad (3)$$

is redundant with "color" conservation. (Reference 15 points out that  $b$  is proportional to hypercharge—the difference between electric charge and the 3-component of isospin—so topological "color" relates to hypercharge.) This feature of "color" has remained unchanged from the quantum-surface representation, as have Feynman rules for "quark-color" switching. In fact all purely strong-interaction Feynman rules<sup>7</sup> are unaffected by the TPT changes proposed in this paper.

We close this section with three remarks.

(1) As with  $f_c$ 's, TPT freezes the orientation of any  $\tau_j$ —a  $\tau$  with at least one end adjacent to a  $j$ . Freezing in the  $c$  direction of hadronic  $\tau_j$  orientations has been long established.<sup>3,4</sup> Reference 17 will explain why nonhadronic  $\tau_j$ 's have orientation frozen in the  $n$  sense.

(2) "Color" lines, although similar in some respects to  $\tau$ 's, always have vertices *inside*  $\Sigma$ ; an  $f_c$  never has *both* ends on the belt, although it may have both ends inside  $\Sigma$ .  $\tau$ 's never terminate inside  $\Sigma$  although they may have points of tangency with other lines.

(3) The continuous sequence of  $f_c$ 's building a "color" line is in 1-to-1 correspondence with some collection of  $f$ 's. (In strong-interaction topologies, this collection forms a continuous sequence.) Even though momentum is

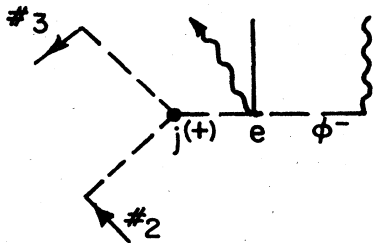


FIG. 14. Lepton  $Y^+, \phi^-$  belt portion.

not transported by a "color" line, a momentum  $p_\mu^i$  attaches to each momentum-copy line. We shall characterize the union of  $F$  with all momentum-copy lines and their linking vertices as the extended momentum graph  $M$  (with lines designated  $\mu$ ).

#### IV. ORIENTED SPINOR AND SCALAR PATCHES

The collection of Feynman lines, "color" lines, and isospin (Finkelstein) lines divide the surface  $\Sigma$  into patches which may be differentiated as either "spinor" or "scalar." What is the topological meaning of such adjectives, which usually associate with behavior of indices in Lorentz transformations? We have seen in Secs. II and III how each color or isospin line inherits a "sense"—expressed through  $(+, -)$  labels on its ends—from the orientation of  $\Sigma$  in conjunction with the Feynman graph. Facing along any  $\tau$  or  $f_c$  in a direction from  $(-)$  to  $(+)$  there is a patch of  $\Sigma$  immediately to the "left" and another immediately to the "right," where left and right are defined by the orientation of  $\Sigma$ . Rather than using these adjectives we choose to employ the terms spinor and scalar, as shown by Fig. 15. Our choice of terminology here stems from the consequence of our rule for  $(+, -)$  indices [e.g., Figs. 3, 4, and 8(b)] that any patch touching a Feynman line is spinor according to Fig. 15. We shall find in Sec. VA that patches adjacent to  $F$  generate indices which transform as spinors under Lorentz transformation. Patches which are scalar according to Fig. 15 never touch  $F$  and do not generate indices involved in Lorentz transformations. Scalar patch-generated indices are discussed in Secs. VC and VD. It is a general TPT principle that the Feynman graph always locates inside a spinor region of  $\Sigma$ . Figure 8(b) (also Figs. 19 and 23) illustrate this principle.

The boundary segments designated by  $\phi$  in Sec. II (Fig. 7) are seen to locate exclusively along the boundaries of spinor patches. We shall find all other  $\beta$ 's to locate exclusively along the boundaries of scalar patches. A characterization of  $\phi$  as "fermionic" and all other  $\beta$ 's as "bosonic" is appropriate when one recalls the  $S$ -matrix connection between spin and statistics established by Stapp.<sup>21</sup> As used in this paper the two adjectives spinor and fermion are to be understood as synonymous—both implying spin- $\frac{1}{2}$  and Fermi statistics. The two adjectives scalar and boson here both imply spin-0 and Bose statistics.

A long-standing TPT postulate has associated chirality with a  $\phi$  label induced by an orientation of the adjacent spinor patch. Section VA will extend the chirality label on  $\phi$ 's to a double label which includes spin, after the present section has given general rules for which  $\Sigma$

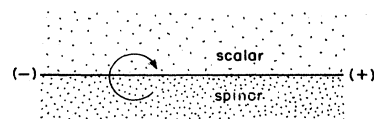


FIG. 15. Separation of scalar from spinor patch by a Finkelstein or "color" line.

patches are to be oriented and how. The notion of  $\phi$  as a fermionic “boundary unit” will be accompanied by two bosonic boundary units, either a single  $\beta$  (Sec. VB) or a Y-shaped  $\beta$  triplet (Sec. VC). We shall associate quark and lepton generation, respectively, with patch-induced labels on these two types of bosonic boundary unit.

Any patch whose boundary includes a  $\beta$  we shall designate as  $\sigma_i$  with boundary  $\partial\sigma_i$ . We orient each  $\sigma_i$  and, independently, each disconnected component  $(\partial\sigma_i)_d$  of  $\partial\sigma_i$ , with these orientations to propagate coherently to the new patch formed when a  $\beta^+\beta^-$  pair is identified and erased in a particle plug. That is, if the symbol  $\sigma_i$  is understood to mean an oriented patch together with its oriented boundary, such a plug amounts to a connected sum

$$\sigma = \sigma' \# \sigma'' .$$

Figure 16 shows the connected sum of a patch  $\sigma'$  that has a single boundary component and a patch  $\sigma''$  that has two boundary components. The indicated orientations are local; the global  $\Sigma$  orientation must simultaneously be perpetuated, as in Fig. 2 (and Fig. 20, below). In this example  $\sigma'$  carries two (local) orientations while  $\sigma''$  and  $\sigma$  both have three orientations. All patches within purely strong-interaction topologies are disks like  $\sigma'$ , with single boundary components and thus two orientations, but Ref. 17 will show purely electroweak topologies to require cylindrical patches like  $\sigma''$ , with two disconnected boundary components and thus three orientations associated with the patch.

Particle quantum numbers will stem from  $\sigma$ -induced labels on  $\partial\Sigma$  “units;” each unit belongs to exactly one boundary component of some  $\sigma$ . The orientation of its  $\sigma$  will endow any  $\partial\Sigma$  unit with one two-valued label and the orientation of its boundary component will supply a second.

All 6 patches of Fig. 3 (3 spinor and 3 scalar) and all 5 patches of Fig. 4 (3 spinor and 2 scalar) are disks, each with a pair of  $\partial\Sigma$  units among boundary segments; each of these  $\sigma$ 's is “doubly oriented.” Figure 8(b) at first sight might appear to contain 12 patches, but one of these (spinor, in the center, bounded entirely by 1  $\tau$  and 2  $\mu$ 's) has no  $\beta$  along its boundary. Such a patch is not a  $\sigma$  and will not be oriented; such a patch will be characterized as “white.” (We shall describe elsewhere how white spinor patches become  $\sigma$ 's when gauge bosons are inserted therein.)

The junction line in Fig. 8(b) further influences the patch structure so as to reduce the number of  $\sigma$ 's; a related effect is the occurrence, at each of the  $J$  ends, of a Y-shaped boundary unit. The requirement that no line in-

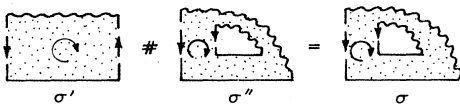


FIG. 16. Connected sum of two patches. Orientation of patch-boundary components is indicated by arrows along  $\beta$ 's (segments of  $\partial\Sigma$ —which lack intrinsic orientation).

side  $\Sigma$  ever touch a  $J$  has always in TPT been accompanied by a rule that local areas of  $\Sigma$  connected by a  $J$ , as well as the boundaries of these areas, are coherently oriented, in the sense of Fig. 17. We maintain these rules and correspondingly speak of a (single)  $\sigma_J$  as any collection of patches (on separate  $\Sigma$  sheets) that touch the same  $J$ . The boundary of any  $\sigma_J$  contains, on a single component, “mated”  $Y^+$  and  $Y^-$   $\partial\Sigma$  units for each bounded  $J$  “within” the  $\sigma_J$ . These two units— $Y^+$  and  $Y^-$ —inherit common labels from the  $\sigma_J$ . The two notions of  $\sigma_J$  and mated  $Y$  boundary units may be captured by thinking of a junction line as lying *inside*  $\sigma_J$  even though it places its mated  $Y^+Y^-$  pair on a *single* boundary component. All  $\sigma_J$ 's are scalar. Examining Fig. 8(b) with the foregoing in mind reveals a total of 9 doubly oriented  $\sigma$ 's, 4 spinor and 5 scalar, one of the latter being a  $\sigma_J$  with a single boundary component.

At this stage we need to describe the “internal” part of  $\partial\Sigma$ , which is entirely fermionic, consisting of  $\phi^+\phi^-$  circular components belonging to *oppositely oriented* spinor  $\partial\sigma$  components. An internal component of  $\partial\Sigma$  contains no  $e$ 's (no  $\pi$ 's) but is tangent to a  $\mu$  and also to a  $\tau$  as shown in Fig. 18; a “gauge hole” here has appeared within  $\Sigma$ . Reference 17 will explain this term. A strong-interaction example of a gauge hole is given in Fig. 19—where 4 external mesons and 1 intermediate meson line appear in a 2-vertex embellished Feynman graph. All 9 patches here are  $\sigma$ 's (5 spinor and 4 scalar) and we have designated by  $\sigma_1$  and  $\sigma_2$  the two spinor patches that touch the internal component of  $\partial\Sigma$ . These two patches are independently oriented but their boundaries are not. The  $\phi^+$  and  $\phi^-$  bounding a gauge hole in  $\Sigma$  always belong to *oppositely oriented*  $(\partial\sigma)_d$ 's; otherwise the hole would be contracted to zero—with two patches becoming a single patch, as in the upper part of Fig. 19.

The patch structure of Fig. 18 arises when the meson plug of Fig. 2 involves a quark-antiquark joining where  $\phi^+$  and  $\phi^-$  belong to oppositely oriented patch boundaries (one clockwise and one anticlockwise) and so may not be identified. See Fig. 20. As reviewed in Sec. VA, the possibility of such mismatches for the fermionic halves of quarks is required by unitarity. In electroweak topologies, as explained by Ref. 17, gauge holes relate to conserved currents (to the maintenance of a zero photon mass).

In Ref. 6 gauge holes were collapsed to “chiral-switch lines” within  $\Sigma$ . (Chiral-switch lines were called “topological gluons” in Ref. 6.) For describing chirality in strong interactions, switch lines and gauge holes are equivalent, but to represent electroweak interactions gauge holes are more convenient.

It has been remarked above that all strong-interaction  $\sigma$ 's are doubly oriented; the orientations of  $\sigma$  and  $\partial\sigma$  here

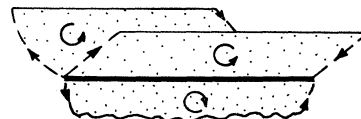


FIG. 17. A junction-line patch  $\sigma_J$ .



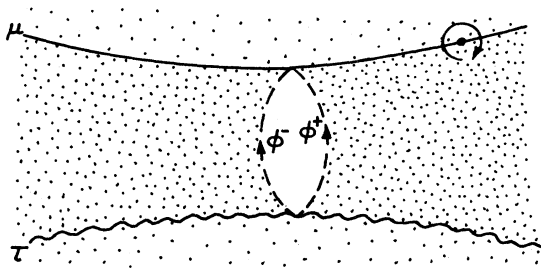


FIG. 18. Gauge hole.

behave in a parallel fashion under connected sums. Either can be represented by an orientation *induced* in a  $\partial\Sigma$  unit. In Ref. 6 only one of the two orientations was recognized and was physically identified for spinor patches with chirality. The chosen orientation was that of a patch but could just as well have been the patch boundary. No attempt was made in Ref. 6 to topologize spin.

Labels attached to a  $\partial\Sigma$  unit depend on *comparing* its  $\sigma$  and  $(\partial\sigma)_d$  orientations to orientations already introduced in Sec. II. We compare  $\sigma$  orientation to global  $\Sigma$  orientation: if these two orientations agree (disagree), we attach a  $U$  ( $D$ ) label to the  $\partial\Sigma$  unit. Global  $\Sigma$  orientation further induces in any  $\partial\Sigma$  unit an orientation to which a  $(\partial\sigma)_d$  orientation can be compared; if these orientations agree (disagree) we attach an  $O$  ( $P$ ) label to the  $\partial\Sigma$  unit. Every boundary unit thereby acquires both a  $(U,D)$  and an  $(O,P)$  label.

V. INTERPRETATION OF LABELS ON BOUNDARY UNITS

A. Spin and chirality

Section II defined a “fermionic”  $\beta$  to be a segment of  $\partial\Sigma$  lying along the boundary of a spinor patch; such a  $\beta$  we have called a  $\phi$ . The present section explains the alge-

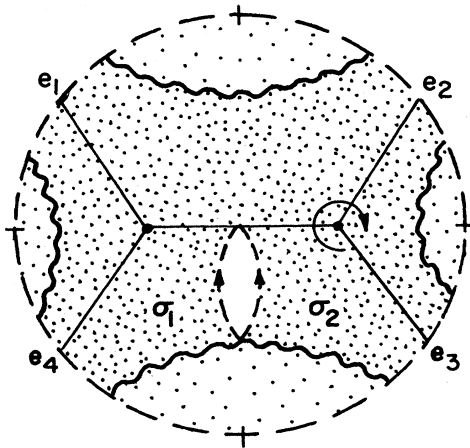


FIG. 19. Gauge hole inside an embellished two-vertex, four-meson Feynman graph.

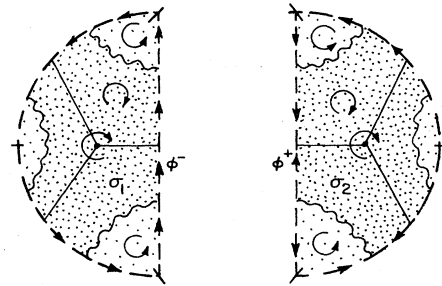


FIG. 20. Two single-vertex, 3-meson embellished Feynman graphs whose connected sum generates the gauge hole of Fig. 19.

braic sense in which a  $\phi$  is a fermion unit.

The  $(U,D)$  and  $(O,P)$  labels on a belt  $\phi$  we propose to interpret, respectively, as spin and chirality. On any  $\phi$  these labels correspond to a Dirac 4-spinor index.  $(U,D)$  associates with spin  $(+\frac{1}{2}, -\frac{1}{2})$  carried by a belt  $\phi$  in the sense of a Stapp  $M$ -function index,<sup>21</sup> while  $O$  [ $P$ ] corresponds in the Weyl basis for Dirac 4-spinors to the “upper” [“lower”] projection  $(1+\gamma_5)/2$  [ $(1-\gamma_5)/2$ ]. Under Lorentz transformations the 4-valued  $(U,D)\times(O,P)$  index on any  $\phi^-$  transforms like  $\psi_\alpha$  while that on any  $\phi^+$  transforms like  $\bar{\psi}_\alpha \equiv (\psi^\dagger \gamma_0)_\alpha$ .

In hadronic belt portions,  $\phi$  units appear exclusively as “halves” of “quarks.” We shall explain in the following paragraphs how the topological proposals of this paper lead to the quark-line Feynman rules of Ref. 7 and give them a detailed representation. As a preliminary we note that a “quark” invariably appears “mated” with an “anti-quark” in a continuous  $4\text{-}\beta$  interval along  $\partial\Sigma$  that begins and terminates at the  $M$  ends touching the mated pair of  $\phi$ 's, but the  $\phi^+$  and  $\phi^-$  may or may not belong to the same  $\sigma$ . In Figs. 3 and 8(b) both members of every mated  $(\phi^+, \phi^-)$  pair belong to the same component of a  $\partial\sigma$ , while in Fig. 19 one of the  $(\phi^+, \phi^-)$  mated pairs along the belt is divided between two oppositely oriented  $\partial\sigma$ 's by a gauge hole in  $\Sigma$ .

If (the belt)  $\phi^+$  and  $\phi^-$  of a quark line belong to the same disk  $\sigma$ , then both carry the *same*  $(O,P)$  and  $(U,D)$  labels; hence the  $4\times 4$  Dirac matrix connecting indices on  $\phi^+$  and  $\phi^-$  is diagonal. Symmetry under reversal of  $\sigma$  and  $\partial\sigma$  orientations then implies a *unit Dirac matrix* in the corresponding Feynman rule. This unit matrix, as discovered independently by Mandelstam<sup>22</sup> and by Stapp,<sup>23</sup> allows topological contraction (“duality”) in the presence of quark spin and chirality; the unit Dirac matrix is central to the algebra of hadronic supersymmetry (Appendix B).

On the other hand, when the  $\phi^+$  and  $\phi^-$  at the ends of a quark line belong to two *different* disks with oppositely oriented boundaries as in Fig. 19, their  $(U,D)$  labels are independent while  $(O,P)$  labels *disagree*. The Feynman rule of Ref. 7, in conformity with Lorentz invariance, uniquely represents the connection between  $\phi^+$  and  $\phi^-$  indices for such a topology by the Dirac matrix (Weyl basis)

$$\not{p}/m_0 = \begin{bmatrix} 0 & \sigma \cdot p/m_0 \\ \bar{\sigma} \cdot p/m_0 & 0 \end{bmatrix}, \quad (4)$$

where  $p$  is the momentum carried by the intermediate Feynman (or momentum-copy) line tangent to the gauge hole separating the two patches (see Fig. 19). The parameter  $m_0$  is the elementary-hadron mass. Reference 17 will generalize such association of a gauge hole with a 4-vector, associating the pair of spin indices on the (nonbelt)  $\phi^+, \phi^-$  bounding the gauge hole with the four values of a Lorentz tensor index.

The full residue of any elementary hadron pole thus gets a familiar Feynman factor  $1 + \not{p}/m_0$  for each quark line that accompanies an intermediate momentum line. Quark lines thereby satisfy the Dirac equation on shell [ $p^2 = m_0^2$ , chirality here being suppressed because  $\frac{1}{2}(1 + \not{p}/m_0)$  is a projection operator], but within the Feynman factor we recognize the unit matrix as representing single disk-patch quark propagation, while  $\not{p}/m_0$  represents two-patch propagation. Unless chirality reverses, spin cannot change. If chirality reverses, spin may or may not change. The foregoing unsymmetrical posture of spin and chirality, implicit in the Dirac "switch" matrix (4), parallels the inequivalent (two- and one-dimensional) manifolds underlying these particle attributes.

Historically, before any topology for spin was introduced, it was understood that Lorentz invariance and unitarity require the switch matrix (4). Once Feynman rules are given (including phase factors for closed loops<sup>23,24</sup>) strong-interaction theory is complete, so readers may wonder why it has been thought necessary to topologize spin. There are two reasons. (1) The theory must be extended *beyond* strong interactions to situations where the Feynman rules remain to be discovered. We anticipate the sole topological repository of *any* particle's spin and chirality to be its  $\phi$  content. (2) Topologizing spin as well as chirality may be a step toward eventually topologizing the full Poincaré group. A continuing defect of TPT is that, although momentum flows through the Feynman graph, there so far has appeared no way to give topological meaning to *quantity* of momentum. Presence of spinor patches on *both* sides of each Feynman line and association of momentum factors with gauge holes invite developments beyond those of this paper.

Reference 17 will discuss a general requirement of Lorentz invariance (going beyond strong interactions) that the boundary of any patch, whether connected or not, either includes no  $\phi$ 's or exactly one  $\phi^+ \phi^-$  pair carrying a single  $(U, D)$  label. Furthermore any  $\partial\sigma$  that includes a  $\phi$  must *not* include  $\beta$ 's other than  $\phi$ 's. We have here another statement that each  $\sigma$  must be purely fermionic or purely bosonic.

### B. Quark generation

A "quark" as defined by Fig. 5 is a  $2\text{-}\beta$  connected belt interval, a (4-spinor, 2-isospinor)  $\phi$  plus a companion  $\beta$  lying along the boundary of a scalar patch and never touching the Feynman graph. Such a belt segment appears only within "quarks" and will be designated  $\delta$ . A  $\delta$  carries no

$(c, n)$  index [no isospin, because its  $(+, -)$  label disagrees with that of the contacting  $\tau$ ] but has a 4-valued  $(U, D) \times (O, P)$  label. We shall designate the label on a  $\delta$  by an index  $G = 1, \dots, 4$  according to Table I.

Disconnection of  $\delta$ 's from  $F$  we interpret as disconnecting  $G$  from Poincaré transformations. In other words we interpret  $G$  when attached to a  $\delta$  as an internal quark degree of freedom, and we call it "topological quark generation." The  $\delta$  boundary unit is bosonic.

The door is open to mixing of topological quark generations when hadrons interact with nonhadrons. In all examples presented in this paper, each  $\delta^-$  is mated with a  $\delta^+$  along the boundary of a disk  $\sigma$  whose orientation is reversible and whose boundary orientation also is reversible. The indices on  $\delta^+$  and  $\delta^-$  are connected in Feynman rules for such topologies by a  $4 \times 4$  unit matrix; there is no breaking of  $G$  symmetry and no  $G$  mixing. But if the two members of a mated  $\delta^+ \delta^-$  pair belong to *different*  $\sigma$ 's, there will be nondiagonal  $4 \times 4$  matrices acting on the quark-generation space and "physical" quark generations will be those (generally inequivalent) linear superpositions of the four topological quark generations that diagonalize these matrices.  $G$  mixing for quarks is probably inconsistent for pure strong interactions and for gauge-boson coupling to hadrons, as will be explained elsewhere, but is plausible in hadron coupling to the  $H$  neutral scalar bosons predicted by TPT (Ref. 25). There is furthermore expectation of coupling between topological quark generation and the lepton generation to be described in Sec. V C.

Notice how the isospin-carrying Finkelstein line in Fig. 5 divides any quark into a fermion half—carrying a 4-valued Dirac index—and a boson half—carrying a 4-valued generation index. Because the fermion half touches  $M$ , the quark Dirac index interacts with momentum and is affected by Lorentz transformations. A lepton (Fig. 14) also divides into a fermion half and a boson half, although the boson half here is a  $Y$  (not a  $\delta$ ), and Sec. V C will reveal four lepton generations corresponding to  $G = 1, \dots, 4$ . Leptons and quarks in TPT bear certain similarities but the parallelism does not go as deep as in standard theory. Because the two halves of a TPT quark are not separated by an  $e$ , a TPT quark does not carry momentum, and because lepton generation associates with a junction line, there will be four separately conserved lepton numbers.  $G$  mixing for quarks is not accompanied by  $G$  mixing for leptons.

The earlier topological representation of quark generation, based on the transverse surface  $\Sigma_Q$ , also corresponded to a 4-valued index because two independent orientations were responsible.<sup>3</sup> Since the transverse surface attached only to hadrons and never played any role in elec-

TABLE I. Topological generation index.

$G$		
1	$O$	$D$
2	$P$	$D$
3	$P$	$U$
4	$O$	$U$

troweak interactions, however, no  $\Sigma_0$  motivation ever was found for quark-generation switching.

### C. Lepton generation

Finally we turn attention to the  $Y$ -shaped boundary unit (Fig. 12) that touches the end of a junction line  $J$ . We have already noted that each mated  $Y^+Y^-$  pair carries a single 4-valued  $(O,P) \times (U,D)$  label. We may designate this label by the symbol  $G$  already defined by Table I; when attached to a  $Y$  as to a  $\delta$ ,  $G$  cannot interact with momentum or undergo Lorentz transformations and therefore represents an internal particle degree of freedom. One reason a  $Y$ , even though contacting  $M$ , is bosonic (scalar) rather than fermionic is because  $G$  is continuously preserved along any junction line; fermionic attributes—spin and chirality—must have capacity to switch.

Defining a quantum number  $b_G$  as the number of  $Y_G^+$  minus the number of  $Y_G^-$ , each of 4  $b_G$ 's is exactly conserved. Our previously defined boson number  $b$  is equal to  $\sum_{G=1}^4 b_G$ . According to Fig. 14 each lepton contains one  $Y^+$ , so each lepton carries +1 unit of a  $b_G$ . To connect  $b_G$  with lepton number for generation  $G$ , it is necessary to recall the “freezing” of all labels on hadronic  $Y$ 's. From the beginning of TPT no degrees of freedom have attached to hadronic  $Y$ 's (Ref. 3), and we do not propose now to tamper with this principle, which will be reviewed below. We extend the convention of Ref. 3 that hadronic  $Y$ 's carry a frozen  $O$  label by requiring them also to carry a frozen  $U$  label. In other words, according to Table I, hadronic  $Y$ 's always carry  $G=4$ . In tabulating elementary-hadron quantum numbers one may ignore the single-valued  $G$  index carried by hadronic  $Y$ 's while recognizing each quark as carrying a 4-valued  $G$  index. At the same time Ref. 17 will stress that lepton coupling to hadrons through junction lines breaks lepton- $G$  symmetry because this coupling is possible only for  $G=4$ .

Even though leptons couple to hadrons through  $G$ , there remains for each  $G$  an absolutely conserved lepton number:

$$L_G \equiv b_G + B\delta_{G4}. \quad (5)$$

Remembering that  $B=0$  for all elementary particle except baryons, and that for hadrons  $b_G = -B\delta_{G4}$ , we see that  $L_G = b_G$  for leptons while  $L_G = 0$  for all hadrons. The previously defined  $G$ -independent lepton number  $L = b + B$  [Eq. (3)] is equal to  $\sum_{G=1}^4 L_G$ .

Notice that the label  $G$  corresponds to physical lepton generation but not to physical quark generation. Physical quark generations are superpositions of different  $G$ 's, and there is no absolutely conserved “quark” number that carries a  $G$  label.

The conserved quantum number  $L_G$  is nonzero not only for leptons but for  $H$  bosons,<sup>25</sup> whose closed  $Y^+Y^-$  belt portion is shown in Fig. 21. Each of these two (nonmated)  $Y$ 's carries a separate  $G$  label. If  $Y^+$  carries  $G'$  and  $Y^-$  carries  $G''$ , then the  $H$  has  $L_{G'} = +1$  and  $L_{G''} = -1$ .

For reasons related to photon masslessness that are explained in Ref. 17, the Finkelstein orientation of any nonhadronic  $Y$  is frozen in the  $n$  sense—nonhadronic  $Y$ 's being electrically neutral. Both hadronic and nonhadronic

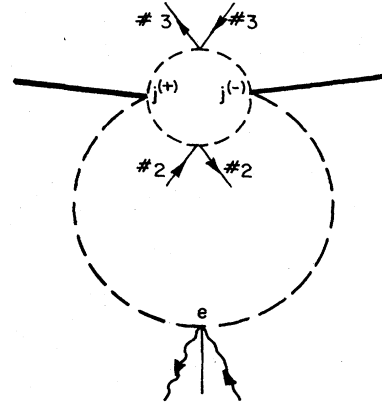


FIG. 21.  $Y^+Y^-$  belt portion of an  $H$  (horizontal) boson. The  $j^{(+)}$  and  $j^{(-)}$  are *not* mated by a junction line.

$Y$ 's touch the extended Feynman graph  $M$  at the ends of all three  $Y$  “legs,” with the end which touches  $F$  also contacting a  $\tau_J$ . The difference between hadronic and nonhadronic  $Y$  lies partly in the opposite  $\tau_J$  orientation and partly in the freezing of hadronic  $(O,P)$  and  $(U,D)$  labels. The latter difference relates to the contractability of zero-entropy hadronic topologies; intermediate elementary hadrons may be indistinguishable from “bound states” of several elementary hadrons while collections of nonhadrons are never equivalent to a single nonhadron. (A nonhadron always is accompanied by nonzero entropy.) Zero-entropy contractions begin by collapsing mated “quark-antiquark”  $\partial\Sigma$  intervals together with the attached  $\sigma$ 's. Rules for such collapse depend entirely on “quark” orientations; hadronic  $Y$ 's are invisible in strong interactions because  $Y^+Y^-$  mated pairs are not adjacent to each other along  $\partial\Sigma$ . Boundary contact between different hadrons occurs exclusively through “quark” content (see Figs. 3 and 8).

No principle has here been proposed forbidding a scalar-patch boundary from including both a  $Y$  and a  $\delta$ . Such inclusion could couple lepton and quark generations and appears natural when  $H$  bosons interact with hadrons; Ref. 17 will provide examples.

Although we now forbid patches of mixed bosonic-fermionic character, such as were employed by Ref. 18 in discussing how parity symmetry can arise from junction lines, a source of parity asymmetry from junction lines has survived through our tying the meaning of  $(O,P)$  indices to orientations of  $\partial\sigma$ 's that may be built partially from  $\tau_J$ 's. Freezing of  $\tau_J$  orientation not only breaks isospin symmetry but now has the potential to break parity symmetry.

## VI. SUMMARY

This paper has simplified topological particle theory (TPT) by restricting Feynman-graph embellishments to a single two-dimensional surface. Strong-interaction Feynman rules have remained unaffected by this change, while quark and lepton generations have been placed on a basis that, although common, forbids lepton-generation mixing

at the same time as allowing generation mixing for “topological quarks.” The four values taken by a generation index have been connected to the four values of a Dirac spinor index, while preserving the scalar (internal) character of the generation index.

Topological representation of isospin has remained unchanged while that of “color” has become similar to that of isospin. [There continues, however, to be no SU(3) “color” symmetry.] The form of TPT proposed here recognizes each elementary particle as “built” from a momentum-carrying Feynman-line end surrounded by three types of “unit”—a fermionic unit  $\phi$  and two bosonic units,  $\delta$  and  $Y$ . Each unit carries a  $(+, -)$  index, which alternates within a particle. Gauge bosons are  $\phi^+, \phi^-$ , leptons (antileptons) are  $Y^+, \phi^-$  ( $\phi^+, Y^-$ ), and  $H$  bosons are  $Y^+, Y^-$ . (The comma here locates the Feynman-line end.) Hadrons are built from  $Y$  units plus “quarks”  $q, a, q$  ( $\bar{q}$ ) being  $\phi^+\delta^-$  ( $\delta^+\phi^-$ ). Mesons are  $q, \bar{q}$ , baryons (antibaryons) are  $q, Y^-qq$  ( $Y^+\bar{q}\bar{q}, \bar{q}$ ), and “hexons” are  $qqY^-, Y^+\bar{q}\bar{q}$  (Ref. 10). A quark, like a lepton, now has a fermion half and a boson half, with generation located in the latter, but a quark continues, as in previous versions of TPT, *not* to carry momentum.

$\phi$  units carry, in addition to a Dirac 4-spinor index, a  $(c, n)$  isospin index.  $Y$  units carry a frozen  $c$  or  $n$  index (this freezing being a source of symmetry breaking) as well as a 4-valued, strictly conserved,  $G$  index.  $\delta$  units carry only a  $G$  index whose conservation may be violated in hadron-nonhadron interactions.

#### ACKNOWLEDGMENTS

The proposals of this paper have been influenced by discussions with F. Capra, B. Dougherty, D. Issler, J. Finkelstein, and H. P. Stapp. The precise topology of spin, in particular, is the result of a suggestion from Stapp. We are indebted to D. Issler for a careful reading of the manuscript. This research was supported in part by the Director, Office of Energy Research, Office of High Energy and Nuclear Physics, Division of High Energy Physics of the U.S. Department of Energy under Contract No. DE-AC03-76SF00098.

#### APPENDIX A: ENTROPY INDICES

For completeness here and in the following appendices we reproduce certain essential TPT ingredients from Ref. 3, with minor adjustments required by the present paper.

An  $S$ -matrix connected part  $M$  is a superposition of amplitudes  $M_\gamma$

$$M = \sum_{\gamma} M_{\gamma}, \quad (\text{A1})$$

each  $M_\gamma$  belonging to an embellished Feynman graph  $\gamma$ . Each  $\gamma$  is characterized by a set  $g_i(\gamma)$  of non-negative integers, called “entropy indices,” which allow terms within the topological expansion (A1) to be ordered according to increasing topological complexity. (The first-appearing  $\gamma$ 's not only have the smallest number of Feynman vertices but the lowest entropy.) Multivertex  $\gamma$ 's are connected sums of single-vertex  $\gamma$ 's

$$\gamma = \gamma' \# \gamma'' \# \dots \quad (\text{A2})$$

In any connected sum an entropy index  $g_i(\gamma)$  cannot decrease and usually increases. Entropy indices exhibit either “strong entropy”

$$g_i(\gamma) \geq g_i(\gamma') + g_i(\gamma'') + \dots \quad (\text{A3})$$

or, at least, “weak entropy”

$$g_i(\gamma) \geq \max[g_i(\gamma'), g_i(\gamma''), \dots] \quad (\text{A4})$$

Four entropy indices  $g_i$  suffice for strong interactions. Two of these,  $g_1$  and  $g_2$ , which we describe as “entropy of the first kind,” were identified already in 1973 by Veneziano<sup>9</sup> and relate to  $\text{th}(F)$ —the infinitesimal thickening of the Feynman graph. The genus of  $\text{th}(F)$  is  $g_1$  while  $g_2$  also depends on genus but further involves the number  $b$  of disconnected components of  $\partial\text{th}(F)$  that contain ends  $e$  of  $F$ :

$$g_2 \equiv g_1 + b - 1. \quad (\text{A5})$$

The index  $g_1$  is “strong” in the sense of (A3) while  $g_2$  is “weak” in the sense of (A4).

An embellished graph  $\gamma$  with  $g_1 = g_2 = 0$  is described as “planar” (graphs with  $g_1 = 0, g_2 = 1$  are called “cylindrical”). Strong-interaction dynamics is dominated by planar  $\gamma$  because of high quark multiplicity. Each quark has a multiplicity  $2^5$  (2 spins, 2 chiralities, 2 isospins, and 4 generations), and only for planar  $\gamma$  can each closed Feynman loop be accompanied by two closed quark loops. The multiplicity of embellished strong-interaction Feynman graphs generally decreases rapidly with increasing  $g_2$ .

The remaining entropy indices,  $g_3$  and  $g_4$ , we describe as “entropy of the second kind.” For strong interactions the index  $g_3$  is the number of gauge holes within  $\Sigma$ , while  $g_4$  is the number of independent Möbius bands within  $\Sigma$ —closed paths which cross junction lines. Both  $g_3$  and  $g_4$  are “strong” and both relate to quark-line complexity. The index  $g_3$  counts the number of “chiral switches” along quark lines while  $g_4$  counts “color switches.” Reference 10 has emphasized that indefinitely large values of  $g_3$  and  $g_4$  make important contributions to strong-interaction dynamics; graph multiplicity does not necessarily decrease with increasing  $g_3$  and  $g_4$ . (According to Ref. 10, entropy of the second kind is responsible for dynamical development of a GeV strong-interaction scale starting from a zero-entropy TeV scale.)

Zero-entropy  $\gamma$ 's—with  $g_1 = g_2 = g_3 = g_4 = 0$ —exhibit a  $2^{10}$  (bosonic)  $\times 2^5$  (fermionic) supersymmetry<sup>26,27</sup> which gradually becomes broken with increasing entropy. Elementary hadrons constitute a zero-entropy supermultiplet (Appendix B). Any embellished graph that includes nonhadrons (external or internal) necessarily has nonzero entropy.

Reference 17 discusses further entropy indices that become significant for nonhadrons. An example is  $g_5$ , defined as the number of nonhadronic Feynman loops.

#### APPENDIX B: ZERO ENTROPY

Contraction rules, unchanged from Ref. 3, imply that any multivertex zero-entropy  $\gamma$  is equivalent to a single vertex. Also unchanged is the rule that any zero-entropy

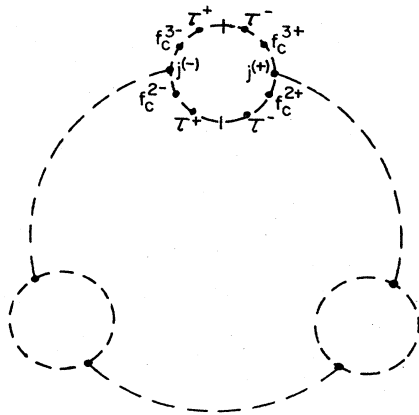


FIG. 22. A 3-beaded zero-entropy belt graph. Only those trivial vertices on one bead are shown.

belt is a “necklace of beads,” a 3-beaded example is given in Fig. 22. Each bead has the same structure—containing no  $e$ 's but along each branch, that connects the bead's mated  $j^+j^-$  pair, there is a mated pair of  $\tau$  ends and a mated pair of  $f_c$  ends. A separate 3-patch (2 scalar, 1 spinor) sheet of  $\Sigma$ , without any portion of  $F$ , belongs to each branch of a zero-entropy bead, as shown by the single-bead zero-entropy example of Fig. 8(b); the “color” lines on the two sheets belonging to the same bead are oppositely oriented.

A typical Feynman-graph carrying zero-entropy sheet,  $S_F$ , corresponding to the three junction lines implied by Fig. 22, is the disk shown in Fig. 23, where spinor and scalar patches are distinguished by different shading. The shading in Fig. 8(b) has the same significance. There are no color lines on a zero-entropy  $S_F$ . It is immediately verifiable that all four entropy indices are zero for the example of Figs. 22 and 23.

The combined content of Figs. 22 and 23 is economically expressible by the shorthand quark-line diagram of Fig. 24, where each “colored” quark line carries a  $2^5$ -valued index. (The color labels in Fig. 24 could be omitted.) Each quark line in Fig. 24 associates with a  $\tau$  (not a  $\tau_j$ ) that

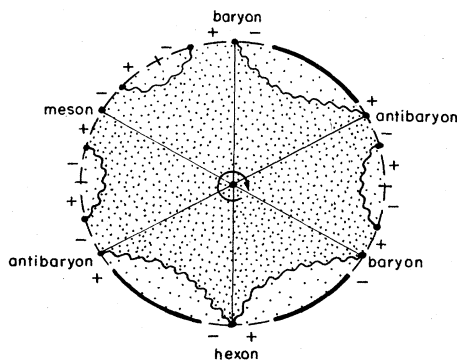


FIG. 23. A zero-entropy sheet embedding a 6-hadron Feynman graph. The belt is that of Fig. 22.

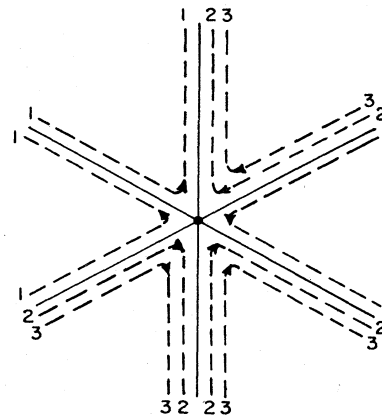


FIG. 24. Shorthand quark-line diagram corresponding to Fig. 23.

connects  $q$  and  $\bar{q}$  intervals of  $\partial\Sigma$ . The arrows on a quark line correspond to the  $(+, -)$  indices on the ends of a  $\tau$  (pointing from  $-$  toward  $+$ ). The Feynman graph could be omitted from the quark-line diagram without loss of information, but we include  $F$  in Fig. 24 to remind readers that TPT quarks do not carry momentum.

Contraction rules imply a single mass  $m_0$  for all elementary hadrons. (According to Ref. 10,  $m_0$  lies in the TeV range.) Figure 25 gives the shorthand representation for the four categories of elementary hadron. Readers should compare Fig. 25 to Figs. 24 and 23 and should note the meaning of “diquark” implied by these figures. The diquark notion is central to TPT hadron dynamics.<sup>10</sup> All strong-interaction embellished Feynman graphs are built by connected sum of zero-entropy  $\gamma$ 's. Strong-interaction Feynman rules are given by Ref. 7 in terms of zero-entropy vertex functions.

APPENDIX C: EMBELLISHED LANDAU GRAPHS

An embellished Landau graph  $L_i^{\gamma', \gamma''}, \dots$  is a connected sum of embellished Feynman graphs  $\gamma', \gamma'', \dots$  not accompanied by erasure of identified  $\partial\Sigma$  segments. Instead the identified segments remain within  $L_i^{\gamma', \gamma''}, \dots$  as *discontinuity lines*. (Discontinuity lines are not patch boundaries.) Figure 26 shows  $L_i^{\gamma', \gamma''}$  for the connected sum of Fig. 20. This example, because of the gauge hole, has nonzero entropy, so the corresponding  $\gamma$  (Fig. 19) is not contractible, while any zero-entropy connected sum (of zero-entropy  $\gamma$ 's) is contractible to a single-vertex  $\gamma$ . Nevertheless, the amplitude  $M_\gamma$  belonging to *any*  $\gamma$ , regardless of entropy content, is an analytic function of momentum with *singularities* which associate with that set of  $L_i^{\gamma', \gamma''}, \dots$  belonging to connected sums which by

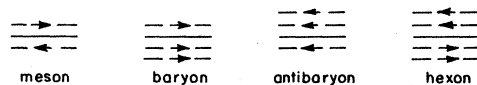


FIG. 25. Shorthand representation of elementary hadrons.

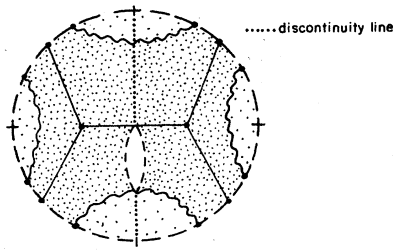


FIG. 26. Embellished Landau graph generated by the connected sum of Fig. 20.

contraction are equivalent to  $\gamma$ . Rules developed by Landau and by Cutkosky associate the location, nature, and strength of each  $M_\gamma$  singularity with some  $L_i^{\gamma, \gamma'}$ , . . . .  $S$ -matrix unitarity is thereby assured, level by level, within the topological expansion (A1).

Landau-Cutkosky rules provide the dynamical equations of zero entropy. The equations are equivalent to planar discontinuity formulas for spinless elementary particles, but for each closed loop of a zero-entropy  $L_i^{\gamma, \gamma'}$ , . . . there is a multiplicity factor  $N_0$ , where

$$N_0 = 2^{10} - 2^5. \quad (C1)$$

Because of Fermi statistics<sup>24</sup> each zero-entropy quark loop brings a factor  $-2^5$  while each diquark loop brings a factor  $(-2^5)^2$ . Figure 27 gives a sample shorthand representation of zero-entropy Landau graphs with quark and diquark loops.

Formula (C1) reveals the need for junction lines in TPT. Without junction lines (and attendant "diquarks")  $N_0$  would be negative and a consistent  $S$  matrix probably could not be achieved, because strong-interaction vertex functions would not be Hermitian analytic.<sup>21</sup> Hermitian analyticity  $M(p) = M^\dagger(p^*)$  is a property of the connected parts of an analytic unitary  $S$  matrix.

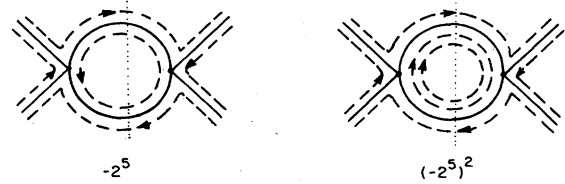


FIG. 27. Shorthand examples of quark and diquark closed loops.

#### APPENDIX D: $P, C, T$

The effect of time reversal, charge conjugation, and parity inversion on a topological amplitude  $M_\gamma$  corresponds to certain orientation reversals. Let  $R$  denote the reversal of *all* orientations, both global and local. Under  $R$  every boundary unit undergoes  $+\leftrightarrow-$  and in  $\leftrightarrow$  out interchange, but all labels,  $(c, n), (O, P), (U, D), (1, 2, 3)$  remain unaltered. If  $R_p$  denotes reversal of all Feynman-line orientations,  $R_p^\sigma$  reversal of all spinor-patch orientations and  $R_p^{\partial\sigma}$  orientation reversal of all spinor-patch boundaries (the subscript  $p$  is a reminder that these orientations relate to the Poincaré group), then

$$P = R_p^{\partial\sigma}, \quad (D1)$$

$$C = RR_p R_p^\sigma, \quad (D2)$$

$$T = RR_p^\sigma R_p^{\partial\sigma}. \quad (D3)$$

It follows that

$$CP = RR_p R_p^\sigma R_p^{\partial\sigma} \quad (D4)$$

corresponds to a reversal of all "non-Poincaré" orientations. It also follows that

$$PCT = R_p. \quad (D5)$$

<sup>1</sup>G. F. Chew, J. Finkelstein, J. P. Surssock, and G. Weissmann, Nucl. Phys. **B136**, 493 (1978).

<sup>2</sup>G. F. Chew, Nucl. Phys. **B151**, 237 (1979).

<sup>3</sup>G. F. Chew and V. Poénaru, Z. Phys. C **11**, 59 (1981).

<sup>4</sup>G. F. Chew, J. Finkelstein, R. M. McMurray, Jr., and V. Poénaru, Phys. Rev. D **24**, 2287 (1981).

<sup>5</sup>J. Finkelstein, Z. Phys. C **13**, 157 (1982).

<sup>6</sup>G. F. Chew and J. Finkelstein, Z. Phys. C **13**, 161 (1982).

<sup>7</sup>G. F. Chew and M. Levinson, Z. Phys. C **20**, 19 (1983).

<sup>8</sup>G. 't Hooft, Nucl. Phys. **B72**, 461 (1974).

<sup>9</sup>G. Veneziano, Nucl. Phys. **B74**, 365 (1974); Phys. Lett. **52B**, 220 (1974).

<sup>10</sup>G. F. Chew, D. Issler, B. Nicolescu, and V. Poénaru, in *Proceedings of the XIXth Rencontre de Moriond, la Plagne,*

*France, 1984*, edited by J. Tran Thanh Van (Editions Frontières, Gif-sur-Yvette, 1984), p. 143.

<sup>11</sup>R. Espinosa, Nuovo Cimento **88A**, 185 (1985).

<sup>12</sup>H. P. Stapp, Phys. Rev. D **28**, 1386 (1983).

<sup>13</sup>G. F. Chew, Phys. Rev. D **27**, 976 (1983).

<sup>14</sup>G. F. Chew and J. Finkelstein, Phys. Rev. Lett. **50**, 795 (1983).

<sup>15</sup>G. F. Chew and J. Finkelstein, Phys. Rev. D **28**, 407 (1983).

<sup>16</sup>G. F. Chew, J. Finkelstein, B. Nicolescu, and V. Poénaru, Z. Phys. C **14**, 289 (1982).

<sup>17</sup>D. Issler (in preparation).

<sup>18</sup>G. F. Chew and V. Poénaru, Phys. Rev. D **30**, 1579 (1984).

<sup>19</sup>H. Harari, Phys. Rev. Lett. **22**, 562 (1969); J. Rosner, *ibid.* **22**, 689 (1969).

<sup>20</sup>G. F. Chew, J. Finkelstein, and D. Issler, Lawrence Berkeley

- Laboratory Report No. 17189, 1983 (unpublished).
- <sup>21</sup>H. P. Stapp, *Phys. Rev.* **125**, 2139 (1962).
- <sup>22</sup>S. Mandelstam, *Phys. Rev. D* **1**, 1745 (1970).
- <sup>23</sup>H. P. Stapp, *Phys. Rev. D* **27**, 2445 (1983); **27**, 2478 (1983).
- <sup>24</sup>C. E. Jones and P. Finkler, *Phys. Rev. D* **31**, 1393 (1985); **31**, 1404 (1985).
- <sup>25</sup>G. F. Chew, J. Finkelstein, B. Nicolescu, and V. Poénaru, *Z. Phys. C* **14**, 289 (1982).
- <sup>26</sup>P. Gauron, B. Nicolescu, and S. Ouvry, *Phys. Rev. D* **24**, 2501 (1981).
- <sup>27</sup>G. F. Chew, *Phys. Rev. Lett.* **47**, 764 (1981).